

Molecular basis of altered excitability in *Shaker* mutants of *Drosophila melanogaster*

Ralf Lichtinghagen, Martin Stocker, Reilinde Wittka², Günther Boheim², Walter Stühmer¹, Alberto Ferrus³ and Olaf Pongs

Ruhr-Universität Bochum, Lehrstuhl für Biochemie, 4300 Bochum, FRG, ¹MPI für biophys. Chemie, Abt. Membranbiophysik, 3400 Göttingen, FRG, ²Ruhr-Universität Bochum, AG Biophys. Chemie von Membranen, Lehrstuhl für Zellphysiologie, 4630 Bochum, FRG and ³Instituto Cajal, 28002 Madrid, Spain.

Communicated by B.Sakmann

Mutations in the *Shaker* (*Sh*) locus of *Drosophila melanogaster* have differing effects on action potential duration and repolarization in neurons as well as on A-type K⁺ channels (*I_A*) in muscle. The molecular basis of three exemplary *Sh* alleles (*Sh*^{KS133}, *Sh*^{E62} and *Sh*⁵) has been identified. They are point mutations in the *Sh* transcription unit expressing aberrant voltage-gated A-type K⁺ channels. Replicas of each mutation have been introduced by *in vitro* mutagenesis into *Sh* cDNA. The expression of *in vitro* transcribed mutant *Sh* cRNA in *Xenopus laevis* oocytes reproduced the specific phenotypic traits of each *Sh* allele. The lack of *I_A* in *Sh*^{KS133} is due to a missense mutation within a sequence motif occurring in all hitherto characterized voltage-gated K⁺ channel forming proteins. The reduction of *I_A* in *Sh*^{E62} is due to a mutation in an AG acceptor site. The intervening sequence between exons 19 and 20 is not spliced in *Sh*^{E62} RNA. As a consequence, *Sh*^{E62} flies do not contain the full complement of *Sh* K⁺ forming proteins. Finally, the *Sh*⁵ mutation leads to an altered voltage dependence of K⁺ channel activation and inactivation as well as to an accelerated rate of recovery from inactivation. This is due to a missense mutation altering the amino acid sequence of the proposed transmembrane segment S5 of the *Sh* K⁺ channels. Segment S5 is located adjacently to the presumed voltage sensor of voltage-gated ion channels. The results explain the altered properties of excitable cells in *Sh* mutants and provide a general model for the possible role of A-type K⁺ channels in modulating action potential profiles.

Key words: action potential/A-current, splicing/potassium channel

Introduction

Action potentials are the rapidly propagated messages that speed along the axons of the nervous system and over the surface of excitable cells. The rising phase of the action potential corresponds to a transient inward current which is usually mediated by a flow of sodium ions through Na⁺ channels. The falling phase of an action potential is mediated by an outward current carried by potassium ions which flow through a variety of K⁺ channels (Hille, 1984). The shape

and frequency of action potentials underlie alterations of synaptic efficiency which in turn leads to an increase or to a reduction in presynaptic neurotransmitter release (Abrams and Kandel, 1988; Cros, 1988). Enhanced neuronal excitability is correlated with cellular events underlying associative learning and memory. In particular, K⁺ channels are involved in alterations of synaptic efficiency. Reduction in the activity of these channels leads to an increase in presynaptic neurotransmitter release reminiscent of a facilitated neurotransmitter release (Abrams and Kandel, 1988; Crow, 1988).

Since the *Shaker* (*Sh*) locus encodes a family of K⁺ channel forming proteins (Iverson *et al.*, 1988; Timpe *et al.*, 1988a,b) *Sh* mutants of *Drosophila melanogaster* are ideally suited to study the molecular basis of altered excitability caused by dysfunctional A-type K⁺ channels. *Sh* mutants have an altered neuronal excitability due to abnormal action potential durations and repolarizations or to abnormal bursts of action potentials (Tanouye *et al.*, 1981; Tanouye and Ferrus, 1985). Also, *Sh* mutants have impaired transient outward K⁺ currents in muscle tissues (Salkoff, 1983; Wu and Haugland, 1985; Solc *et al.*, 1987).

We have characterized three particular *Sh* mutants (*Sh*^{KS133}, *Sh*^{E62}, *Sh*⁵) which are point mutations within the K⁺ channel transcription unit. Each *Sh* mutant exhibits distinct alterations in the action potential profile measured in the cervical giant interneurons of *D. melanogaster*. The allele *Sh*^{KS133} shows action potentials with a long delay in their repolarization (Tanouye and Ferrus, 1985). In addition, A-channels in *Sh*^{KS133} muscle fibres appear to be absent (Solc *et al.*, 1987). *Sh*^{E62} mutants exhibit repetitive, albeit irregular firing of action potentials (Tanouye and Ferrus, 1985) and a residual *I_A* in muscle fibres (Timpe and Jan, 1987). Finally, the allele *Sh*⁵ causes repetitive firing of burst shaped action potentials (Tanouye and Ferrus, 1985). *I_A* in muscle fibres is shifted to more positive potentials (Wu and Haugland, 1985) and the rate of recovery from *I_A* inactivation is accelerated (Salkoff, 1983).

Replicas of the mutants were introduced into cDNA by *in vitro* mutagenesis, in order to correlate the structural alteration in the mutant *Sh* K⁺ channel with the altered A-currents in muscle cells as well as with the altered action potential profiles in interneurons of *Sh* mutants. The cDNA replicas of the *Sh* mutants were transcribed *in vitro* into cRNA, the expression of which was studied after injection into *Xenopus laevis* oocytes. Properties of the mutant *Sh* K⁺ channels were compared with those of wild type *Sh* K⁺ channels. The results show that phenotypic traits which have been described for each *Sh* mutant under study were reproduced in the *X. laevis* oocyte expression system. Thus, the abnormal excitability of *Sh* mutants is caused by structural defects in *Sh* K⁺ channel forming proteins. Implications of these results are discussed in the light of the role of A-type K⁺ channels in modulating and shaping action potential profiles.

Results

The members of the K^+ channel family which is encoded in the *Shaker* (*Sh*) locus share a common core region flanked by variant N- and C-terminal sequences (Kamb *et al.*, 1988; Pongs *et al.*, 1988; Schwarz *et al.*, 1988). Therefore, two principally different types of mutations can occur within the coding region of the *Sh* transcription unit. Mutations alter either a sequence encoding one of the variant terminal ends or the sequence which encodes the core region of the K^+ channel forming proteins. In the former case, only some members of the K^+ channel family should be dysfunctional, whereas in the latter case the entire K^+ channel family should have lost or altered its activity. Previously, we have shown that *Sh*¹⁰² mutation is a nonsense mutation in the *Sh* core region causing the production of truncated K^+ channel subunits (Gisselmann *et al.*, 1989). This leads to a strong dominant *Sh* phenotype. The mutations *Sh*¹⁰² and *Sh*^{KS133} should reside in close proximity since they have not been

separated by recombination (Kamb *et al.*, 1987; Ferrus *et al.*, 1990). Therefore, we entertained the hypothesis that the *Sh*^{KS133} mutation also resides in the *Sh* core region not far from the *Sh*¹⁰² mutation. A *Sh*^{KS133} genomic DNA library was constructed and the exons encoding the core region were subcloned and sequenced. The comparison of the *Sh*^{KS133} DNA sequence with that of the parental Canton S chromosome indicated a single base change (T to A) in exon 15 (Figure 1A). As a result, the derived *Sh*^{KS133} proteins would have the amino acid aspartic acid (GAT) instead of valine (GTT) (Figure 1B). The *Sh*^{KS133} missense mutation is located within the bend region connecting the proposed membrane spanning segments S5 and S6 (Figure 1C) according to the topological model of K^+ channel subunits (Pongs *et al.*, 1988). Thus, the *Sh*^{KS133} and *Sh*¹⁰² mutations are only separated by a small distance (27 bp) on the chromosome.

Electrophysiologically, *Sh*^{KS133} flies lack the A-type K^+ current in muscle (Wu and Haugland, 1985; Solc *et al.*, 1987) and have abnormally prolonged action potentials in interneurons (Tanouye and Ferrus, 1985) suggesting that the *Sh*^{KS133} mutation leads to non-functional K^+ channels. This proposition was tested in the *X.laevis* oocyte expression system. A replica of the *Sh*^{KS133} mutation was introduced into *ShA2* cDNA (for nomenclature see Baumann *et al.*, 1989 and Materials and methods). After injection into *X.laevis* oocytes the expression of *in vitro* transcribed *ShA2* cRNA (Figure 2) mediates a rapidly inactivating A-type K^+ current (Iverson *et al.*, 1988; Timpe *et al.*, 1988a,b). Whereas several independent injections ($n = 15$) for three different *ShA2* cRNA preparations always resulted in the expression of the expected rapidly inactivating A-type current, injections ($n = 13$) of three different *Sh*^{KS133}*A2* cRNA preparations did not elicit a measurable outward (K^+) current (Figure 2). Genetically, the *Sh*^{KS133} mutation behaves like an antimorph (Ferrus *et al.*, 1990). The mutation cannot be compensated in gene dosage experiments by adding extra doses of the *Sh*⁺ locus. The most likely explanation for this behaviour is that mutated *Sh*^{KS133} K^+ channel subunits assemble into multimeric, aberrant non-functional potassium channels (Gisselmann *et al.*, 1989). This hypothesis was tested by coinjecting various mixtures of *ShA2* and *Sh*^{KS133}*A2* cRNA into *X.laevis* oocytes (Figure 2). I_A peak amplitudes were measured after each injection using the same amount of cRNA being either *ShA2* cRNA alone, a 1:1, a 3:1 and a 5:1 mixture of *ShA2* and *Sh*^{KS133}*A2* cRNAs or *Sh*^{KS133}*A2* cRNA alone. In comparison with the *ShA2* cRNA injections, the ones of 1:1 mixtures of *ShA2* cRNA and *Sh*^{KS133}*A2* contained 50% of the original amount of *ShA2* and so forth. In control experiments, measured I_A peak amplitudes were proportional to the amount of injected *ShA2* cRNA (data not shown; comparable control experiments are shown in Figure 5). If the expression of *Sh*^{KS133}*A2* cRNA would not interfere with the expression of *ShA2* cRNA, the injection of 1:1 mixture of *ShA2* and *Sh*^{KS133}*A2* cRNAs should have given ~50% of the original I_A peak amplitude obtained after injecting *ShA2* cRNA alone. Accordingly, the injection of 3:1 mixture should have given ~75% of the original peak amplitude and the one of a 5:1 mixture ~83%. In fact injections ($n = 22$) of a 1:1 mixture of *ShA2* and *Sh*^{KS133}*A2* cRNAs gave ~20% of the expected I_A amplitude (Figure 2); injections ($n = 31$) of a 3:1 mixture of *ShA2* and *Sh*^{KS133}*A2* cRNAs gave ~55% and those (n

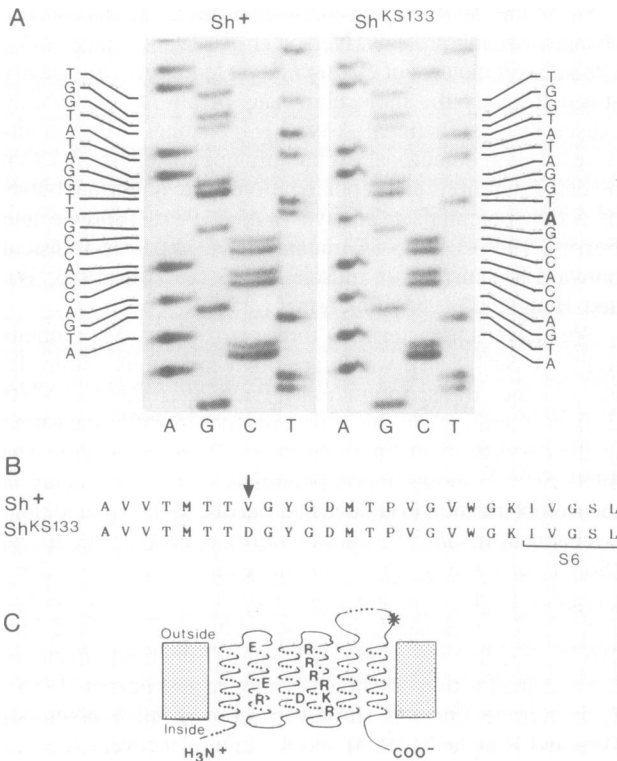


Fig. 1. Molecular basis of the mutation in *Sh*^{KS133} flies. (A) Part of the exon 15 sequence of the *Sh* transcription unit of Canton S DNA (*Sh*⁺) and of *Sh*^{KS133} DNA. The sequence corresponds to nucleotides 1276–1296 of *Sh* β cDNA (Pongs *et al.*, 1988). The T to A base change between wild type and mutant DNA is emphasized by a bold A in the *Sh*^{KS133} sequence on the right hand side. Wild type DNA of the *Sh* locus has been isolated and sequenced as described previously (Pongs *et al.*, 1988). (B) Comparison of the derived *Sh*⁺ and *Sh*^{KS133} amino acid sequences. The sequence is given in the standard one letter code. The sequence corresponds to amino acids 422–447 in *ShA2* protein (*ShA2* is equivalent to *ShB*, Schwarz *et al.*, 1988). The replacement of valine (V) by aspartic acid (D) in *Sh*^{KS133} proteins is indicated by an arrow and the beginning of proposed transmembrane segment S6 by a bracket. (C) Topological model of a *Sh* potassium channel subunit (Pongs *et al.*, 1988) inserted into the membrane having the N- and C-termini on the cytoplasmic side of the membrane. Charged amino acids within the six proposed transmembrane helices are indicated (D, aspartic acid; E, glutamic acid; K, lysine; R, arginine). The asterisk in the model illustrates the location of the missense mutation in *Sh*^{KS133} K^+ channel subunits.

= 21) of a 5:1 mixture ~73% of the expected I_A amplitude (Figure 2). These results, obtained by studying the expression of Sh^{KS133} cRNA in *X.laevis* oocytes, are in harmony with the genetic and electrophysiological properties of Sh^{KS133} mutants. Therefore, we conclude that the molecular basis of the Sh^{KS133} phenotype is the missense mutation in the bend region connecting proposed transmembrane segments S5 and S6 of the $Sh K^+$ channel proteins (see Figure 1).

The Sh^{E62} mutation has been mapped genetically distal to the Sh^{KS133} mutation (Kamb *et al.*, 1987; Ferrus *et al.*, 1990). Therefore, the Sh^{E62} mutation should reside somewhere at the edge of the Sh core region (exon 15) or even further downstream in exons 16–18 or 19–21, which encode the two alternative C-termini of $Sh K^+$ channel proteins (Pongs *et al.*, 1988). Action potentials in Sh^{E62} interneurons are irregular, but are not broadened like the ones in Sh^{KS133} interneurons (Tanouye and Ferrus, 1985). Also, I_A is not eliminated in muscle, but the peak amplitude is significantly smaller than in wild-type (Timpe and Jan, 1987). A Sh^{E62} genomic DNA library was constructed. The two alternative 3'-ends of the Sh^{E62} transcription unit (exons 16–21) were sequenced. Comparison of the Sh^{E62} sequence with that of the parent chromosome indicated one base change (G to A) (Figure 3A). As a consequence, the wild type AG acceptor site sequence at the intron/exon 20 border has been mutated to the sequence AA (Figure 3B). In fact, the Sh^{E62} mutation moves the AG acceptor site by one base pair into the open reading frame of exon 20. Therefore this mutation would alter the processing of Sh mRNA. The two most probable possibilities are: (i) the intron between exons 19 and 20 is not spliced; (ii) the intron between exons 19 and 20 is spliced incorrectly. In the former case, the Sh^{E62} mRNA should contain the intervening sequence between exon 19 and exon 20; in the latter case, the Sh^{E62} mRNA should have a size like Sh^+ mRNA and would contain a

coding sequence with a frame-shift mutation. The two possibilities were distinguished by investigating Sh^+ and Sh^{E62} mRNA in a polymerase chain reaction (PCR) (Saiki *et al.*, 1988). Sh mRNAs were transcribed *in vitro* into cDNAs. They were used as templates in a PCR reaction primed with one primer, complementary to exon 19, and with a second one, complementary to exon 21, as illustrated in Figure 4A. The amplification products (Figure 4B) were subcloned and sequenced. The three anticipated sizes of the amplification products were: (i) 1.2 kb, if the introns between exons 19/20 and 20/21 were not spliced, (ii) 0.8 kb, if only the intron between exons 19 and 20 were not spliced, (iii) 0.58 kb, if Sh^{E62} mRNA was spliced similarly to Sh^+ mRNA. The 1.2 kb amplification product was only obtained in a PCR reaction with Sh^{E62} genomic DNA as template (lane 1 in Figure 4B). On the other hand, the 0.58 kb amplification product was only obtained with Sh^+ mRNA as starting material, whereas Sh^{E62} mRNA yielded the 0.8 kb amplification product corresponding to the sequence shown in Figure 3B. This sequence contained the intervening sequence between exon 19 and exon 20. The sequence was identical to that of Sh^+ DNA except for the mutation in the acceptor site AG (Figure 3A). These results demonstrate that the intervening sequence between exons 19 and 20 is not spliced in Sh^{E62} mRNA because of a mutation in the acceptor AG sequence and not because of a mutation elsewhere. The derived protein sequence of the unspliced Sh^{E62} mRNA (Figure 3C) indicates that the mutation leads to an aberrant C-terminus. The predicting reading frame terminates at a stop codon within the intervening sequence between exon 19 and exon 20. Thus Sh^{E62} proteins are lacking the last 103 amino acids of the corresponding wild type protein sequence.

We investigated whether the deficient C-terminus in Sh^{E62} proteins affects the electrophysiological properties of

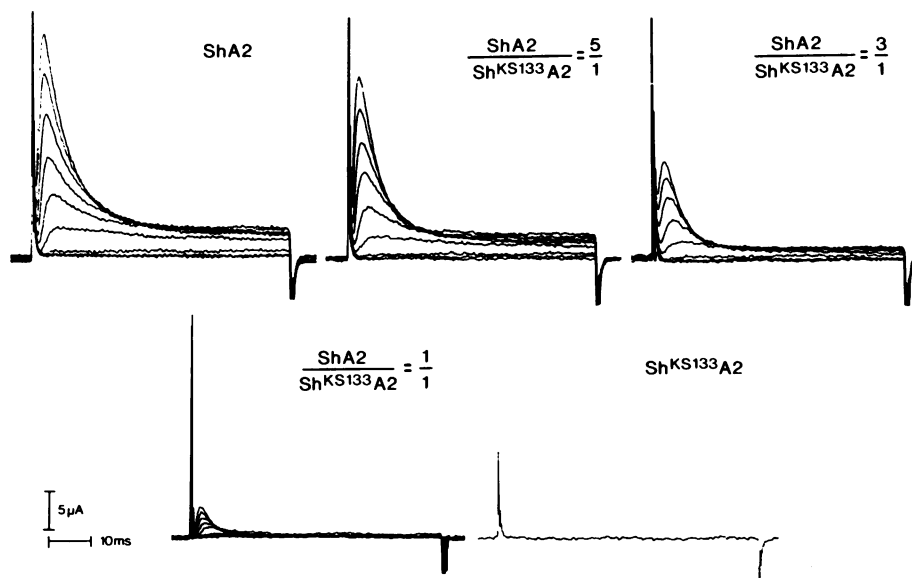


Fig. 2. Expression of transient outward currents in *X.laevis* oocytes injected with $ShA2$ and $Sh^{KS133}A2$ cRNAs synthesized *in vitro*. Outward currents were recorded in a two electrode voltage clamp configuration. Membrane currents were elicited by potential steps from -80 mV to levels between -50 mV and $+20$ mV, in 10 mV increments. Leak currents have been subtracted. Representative current records are shown which were obtained (from left to right and from top to bottom) after the injection into *X.laevis* oocytes of $ShA2$ cRNA ($ShA2$), of a 5:1 mixture, of a 3:1 mixture, of a 1:1 equimolar mixture of $ShA2$ and $Sh^{KS133}A2$ cRNAs and of $Sh^{KS133}A2$ cRNA. Mean amplitudes at $+20$ mV test potentials were for $ShA2$ currents $31.4 \pm 26.7 \mu A$ ($n = 15$), for $ShA2-Sh^{KS133}A2$ (5:1) currents $19.1 \pm 12.8 \mu A$ ($n = 21$), for $ShA2-Sh^{KS133}A2$ (3:1) currents $12.5 \pm 7.8 \mu A$ ($n = 31$), and for $ShA2-Sh^{KS133}A2$ (1:1) currents $3.4 \pm 3.5 \mu A$ ($n = 22$). $Sh^{KS133}A2$ cRNA injections ($n = 13$) did not elicit a measurable current.

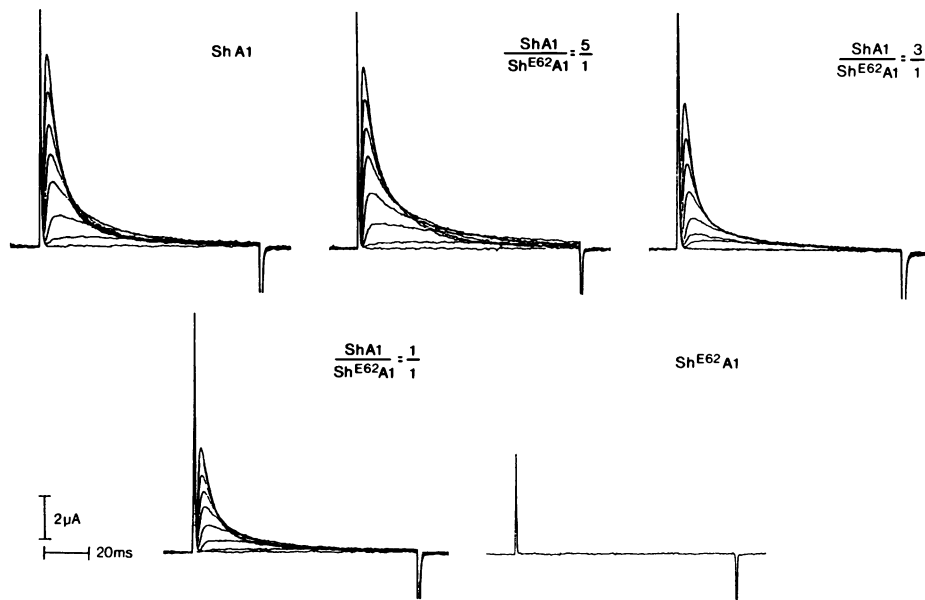


Fig. 5. Expression of transient outward currents in *X.laevis* oocytes injected with *ShA1* and *Sh^{E62A1}* cRNAs synthesized *in vitro*. Outward currents were recorded in a two electrode voltage clamp configuration. Membrane currents were elicited by potential steps from -80 mV to levels between -50 mV and $+20$ mV, in 10 mV increments. Leak currents have been subtracted. Representative current records are shown which were obtained (from left to right and from top to bottom) after the injection into *X.laevis* oocytes of *ShA1* cRNA (*ShA1*), of 5:1 mixtures, of 3:1 mixtures, of 1:1 mixtures of *ShA1* and *Sh^{E62A1}* cRNAs and of *Sh^{E62A1}* cRNA (*Sh^{E62A1}*). Mean amplitudes at $+20$ mV test potentials were for *ShA1* currents 14.7 ± 7.6 μ A ($n = 28$), for *ShA1*–*Sh^{E62A1}* (5:1) currents 11.2 ± 6.1 μ A ($n = 20$), for *ShA1*–*Sh^{E62A1}* (3:1) currents 9.7 ± 4.3 μ A ($n = 21$) and for *ShA1*–*Sh^{E62A1}* (1:1) currents 7.8 ± 3.8 μ A ($n = 24$). *Sh^{E62A1}* cRNA injections ($n = 21$) did not elicit a measurable current.

(Tanouye and Ferrus, 1985). The *Sh⁵* mutation could not be separated genetically from the *Sh^{K5133}* mutation (Ferrus *et al.*, 1990). We hypothesized that this mutation also affects the sequence of the *Sh* core region. A *Sh⁵* genomic DNA library was constructed and the *Sh* core region was sequenced. Only one sequence alteration was discovered between the core region sequence of the parent Canton S chromosome and *Sh⁵* DNA (Figure 6A). The detected base change (T to A) in exon 14 represents a missense mutation, which replaces in the predicted *Sh* protein sequences a phenylalanine (TTT) by an isoleucine (ATT) (Figure 6B). This isoleucine is located in the topological model proposed for *Sh* protein within the putative transmembrane segment S5 as indicated in Figure 6C. The missense mutation is apparently the molecular basis of the *Sh⁵* phenotype. This proposition was again tested in the *X.laevis* oocyte expression system.

A replica of the *Sh⁵* mutation was introduced *in vitro* into *ShA2* cDNA. Injections of *in vitro* transcribed *ShA2* or the *Sh⁵A2* cRNA in *X.laevis* oocytes gave rise to similar transient outward currents (Figure 7A). In order to compare in greater detail the time course and voltage dependence, currents were recorded from macro-patches on *X.laevis* oocytes. Normalized conductance voltage relations of the currents indicate that they activate at test potentials of -40 mV (Figure 7B). However, the voltage dependence of activation for the *Sh⁵A2* K^+ channels was less steep than the one for *ShA2* K^+ channels. Consequently, *Sh⁵A2* I_A reaches the half-maximal conductance at ~ 7 mV more positive potentials (Table I). This result is comparable with the change in voltage dependence of I_A found in muscle of *Sh⁵* larvae (Wu and Haugland, 1985; Zagotta and Aldrich, 1990), where voltage dependence of I_A activation is shifted ~ 10 mV to more positive levels. Moreover, the rates of I_A activation were different between *ShA2* and *Sh⁵A2* currents (Table I). The rise to peak current from a holding

potential of -80 mV to a test potential of 0 mV required 1.4 ms for *ShA2* currents and 0.9 ms for *Sh⁵A2* currents. The voltage dependence of prepulse inactivation of *Sh⁵A2* currents was also altered. *ShA2* and *Sh⁵A2* currents were completely inactivated at a test potential of -40 to -30 mV, but the steepness of the voltage dependence of prepulse inactivation was altered in the case of *Sh⁵A2* (Table I). Similar differences in slopes of e -fold/mV for *Sh⁺* and *Sh⁵* K^+ channels have been reported using whole cell recording techniques on cultured embryonic myotubes from *Drosophila* (Zagotta and Aldrich, 1990). The acceleration of the rate of recovery from I_A inactivation in muscle of *Sh* pupae is most notable in experimental protocols using prepulse potentials of -50 mV (Salkoff, 1983). In the oocyte expression system, the difference between the rates of recovery from *ShA2* and *Sh⁵A2* I_A inactivation was largest when potentials of -40 mV were used (Table I). Under these experimental conditions, *Sh⁵A2* currents recovered from inactivation twice as fast as *ShA2* currents. A detailed description of these experiments will be published elsewhere.

In contrast to the gating behaviour, the single channel conductance of *Sh* K^+ channels was not significantly altered by the *Sh⁵* mutation (Table I). *ShA2* as well as *Sh⁵A2* unitary currents are binomially distributed around a mean of 0.71 and 0.78 pA giving an apparent single-channel conductance of 7.1 and 7.8 pS, respectively (Table I). Open duration histograms of *ShA2* and *Sh⁵A2* channels at 0 mV are well fitted by single exponential probability density functions with a mean time constant of 1 ms (data not shown). Also the pharmacology of *ShA2* and *Sh⁵A2* K^+ channels was comparable (Table II). *Sh⁵A2* channels were slightly more sensitive to 4-aminopyridine (4-AP) and to tetraethylammonium chloride (TEA). Both channels had the same sensitivity or insensitivity towards the toxins charybdotoxin (CTX), dendrotoxin (DTX) and mast cell degranulating peptide (MCDP), respectively.

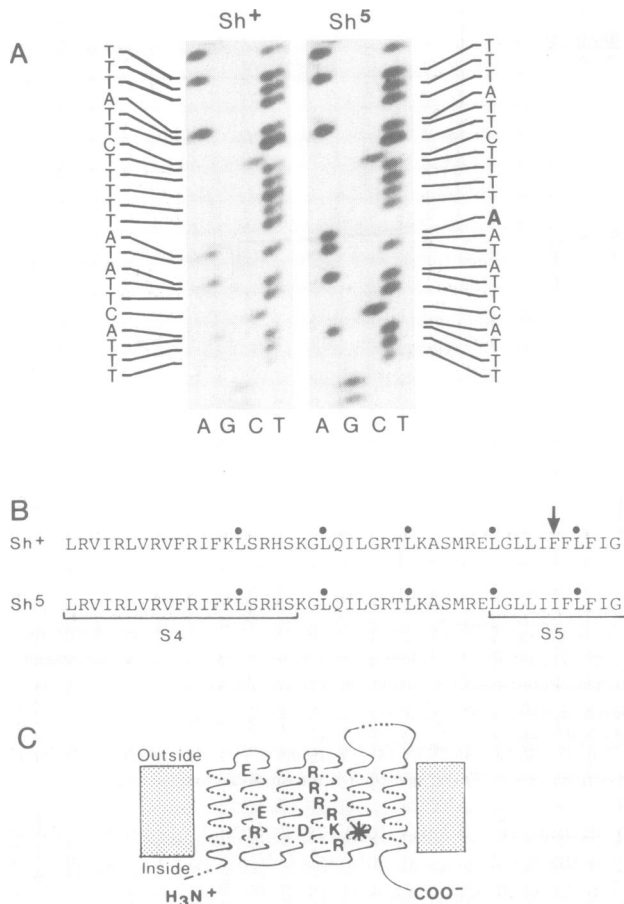


Fig. 6. Molecular basis of the mutation in *Sh*⁵ flies. (A) Sequence of part of exon 14 of the *Sh* transcription unit of Canton S DNA (*Sh*⁺) and of *Sh*⁵ DNA (*Sh*⁵). The sequence corresponds to nucleotides 1149–1170 of *Sh* β cDNA (Pongs *et al.*, 1988). The T to A base change between wild type and mutant DNA is emphasized by a bold A in the *Sh*⁵ sequence on the right hand side of the *Sh*⁵ sequencing gel. (B) Comparison of the derived *Sh*⁺ and *Sh*⁵ amino acid sequences. The sequence is given in the standard one letter code and corresponds to amino acids 347–392 in *ShA2* protein (*ShA2* is equivalent to *ShB*, Schwarz *et al.*, 1988). The replacement of phenylalanine (F) by isoleucine (I) in *Sh*⁵ proteins is indicated by an arrow. Proposed transmembrane segments S4 and S5 (Pongs *et al.*, 1988) are underlined by brackets. Dots on top of the amino acid leucine denote a heptad repeat of five leucines indicative of a leucine zipper motif (McCormack *et al.*, 1989). (C) Topological model of a *Sh* K⁺ channel subunit (Pongs *et al.*, 1988) inserted into the membrane having the N- and C-termini on the cytoplasmic side of the membrane. The asterisk in proposed transmembrane segment S5 indicates the site of the missense mutation in *Sh*⁵ K⁺ channel subunits. Charged amino acids within segments S2, S3, and S4 are indicated (D, aspartic acid; E, glutamic acid; K, lysine; R, arginine).

Discussion

Sh mutants and neuronal excitability

The molecular basis of three *Sh* mutants has been clarified in this report. Replicas of three mutations have been introduced *in vitro* into *ShA1* or *ShA2* cDNA, respectively. The expression of the cRNAs after injection into *X.laevis* oocytes was studied. The results show that phenotypic traits which have been described for each *Sh* mutation under study were reproduced satisfactorily in the *X.laevis* oocyte expression system. The abnormal neuronal excitability of the *Sh* mutants can now be correlated with structural defects in *Sh* K⁺ channel subunits. Basically, three different types of action potentials are seen in *Sh* mutant *Drosophila*. In

each case, abnormalities are limited to action potential repolarization. Different alleles, however, cause differing delayed repolarization and increased action potential durations (Tanouye and Ferrus, 1985). The action potentials of *Sh*^{K^{S133}} and *Sh*¹⁰² have durations increased by a factor of 10 or more, when compared with normal. These two mutants also appear to be the most vigorous leg shakers. They represent extreme forms of the *Sh* defect because in both cases the core region of the *Sh* K⁺ channels is mutated. Whereas *Sh*^{K^{S133}} is a missense mutation (Figure 1), *Sh*¹⁰² is a nonsense mutation (Gisselmann *et al.*, 1989) within the core region. These two mutations affect all K⁺ channel forming *Sh* proteins. Both *Sh* mutants behave as antimorphs in gene dosage tests (Salkoff, 1983; Ferrus *et al.*, 1990). This behaviour must be due to the interference of non-functional *Sh*^{K^{S133}} or *Sh*¹⁰² A-channel subunits with their normal counterpart according to our previous results with *Sh*¹⁰² transformants (Gisselmann *et al.*, 1989) and the *Sh*^{K^{S133}}A2–*ShA2* cRNA expression studies in this report. These data suggest that the mutant *Sh* K⁺ channel subunits assemble together with wild type subunits into multimers which cannot function as K⁺ channels. In this context it should be noted, that Western blot analysis of membrane proteins of *Sh*^{K^{S133}} flies with *Sh* K⁺ channel antibodies has indicated that the mutant *Sh*^{K^{S133}} K⁺ channel protein is inserted into neuronal membranes (Barbas *et al.*, 1989).

Sh^{E62} is a weak *Sh* allele, where action potentials are moderately increased (by a factor of 2–3) compared with normal (Tanouye and Ferrus, 1985). In this case, the mutation does not reside in the core region of *Sh* proteins. Only one of the alternative C-termini in the *Sh* protein family is affected. Thus, some, but not all members of the *Sh* protein family are non-functional. This observation is in good agreement with the *Sh*^{E62} phenotype which behaves like a hypomorph (Timpe and Jan, 1987).

Our results suggest that a mutation in the proposed transmembrane segment S5 of *Sh*⁵ K⁺ channels is responsible for the generation of multiple spikes following the initial incomplete repolarization of action potentials (Tanouye and Ferrus, 1985). However, it is not clear at present how the abnormal gating behaviour of *Sh*⁵ K⁺ channels (Zagotta and Aldrich, 1990) releases *Drosophila* interneurons to fire repetitively.

Sh mutants and I_A in muscle

The replication of aberrant *Sh* K⁺ channels in the oocyte expression system also provides the molecular basis of altered I_A observed in muscle cells of *Sh* mutants (Wu and Haugland, 1985). We have clarified why muscle cells in *Sh*^{K^{S133}} flies lack active *Sh* K⁺ channels. In addition, we have shown that a single point mutation is responsible for the various alterations which have been reported for I_A in muscle of *Sh*⁵ larvae (Wu and Haugland, 1985) and pupae (Salkoff, 1983). Similar alterations in the voltage dependence of activation and inactivation and also in the rate of recovery from I_A inactivation were observed in the oocyte expression system with the *ShA2* member of the *Sh* K⁺ channel family. Presently, we do not know whether this particular member of the *Sh* K⁺ channel family constitutes the *Sh* K⁺ channel in muscle. However, we presume that all members of the *Sh* K⁺ channel family are similarly affected by the *Sh*⁵ mutation, since it has occurred in the core region of the *Sh* transcription unit.

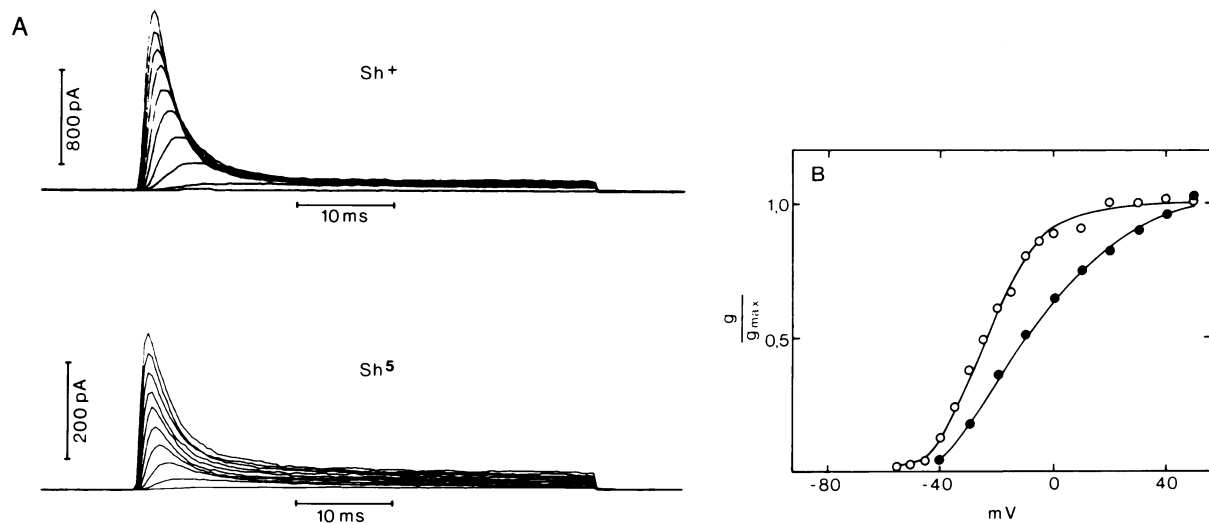


Fig. 7. Expression of transient outward currents in *X.laevis* oocytes injected with *ShA2* or *Sh⁵A2* cRNA. (A) Outward currents recorded in oocytes injected with *ShA2* or *Sh⁵A2* cRNA through a macro-patch in the cell-attached configuration. Membrane currents evoked by potential steps from -100 mV to levels between -60 mV and $+40$ mV, in 10 mV increments are shown. Leak and linear capacitive currents, determined from hyperpolarizing steps, have been subtracted. (B) Normalized conductance–voltage relations of the *ShA2* ($-\circ-$) and *Sh⁵A2* ($-●-$) currents. Peak conductances were calculated from the experiments in A according to equation $g = I_p / (V_m - V_r)$ in which I_p is the peak current, V_m is the membrane potential during the step, and V_r is the reversal potential of the A-current. Peak conductances were normalized to the maximum conductances. The average reversal potential was assumed to be -100 mV.

Table 1. Functional characteristics of *Sh⁵A2* and *ShA2* channels expressed in *X.laevis* oocytes following injection of cDNA

cRNA type	Activation			Inactivation		Single channel currents $i(0)$ (pA) ^f	Recovery from inactivation τ (ms) ^g
	$V_{1/2}^n$ (mV) ^a	a_n (mV) ^b	t_n (ms) ^c	$V_{1/2}^n$ (mV) ^d	a_n (mV) ^e		
<i>ShA2</i>	-14.5 ± 9.8 (9)	13.6 ± 2.1 (9)	1.4 ± 0.5 (9)	6.6 ± 0.9 (2)	3.9 ± 0.6 (2)	0.71 ± 0.13	66.1 ± 2.5 (3)
<i>Sh⁵A2</i>	-7.8 ± 7.6 (7)	17.4 ± 2.5 (7)	0.9 ± 0.2 (7)	8.8 ± 0.9 (7)	2.9 ± 0.3 (7)	0.78 ± 0.11	36.63 ± 6.6 (2)

Numbers in parenthesis refer to number of experiments.

^aRefers to test potential in mV where the conductance increase has reached one-half of its maximal value. The conductance was calculated for each test potential by dividing the current amplitude by the driving force. The potassium reversal potential was estimated to be -100 mV. Ensemble current recording from macro-patches. Voltage steps were made from -80 mV holding potential.

^bRefers to slope of normalized conductance–voltage relation. Its value corresponds to the change in test potential (in mV) to cause an e -fold increase in conductance.

^cRefers to rise time of ensemble patch currents in ms. It was measured at $+10$ mV test potential following step changes from -80 mV membrane potential. The rise refers to the time the current rises from 10 to 90% of its final value.

^dRefers to prepulse membrane potential in mV at which the current response to a step to 0 mV test potential is 50% of its maximal value. Prepulse duration is 1 s. Holding potential -80 mV. Ensemble currents were recorded from macro-patches in the cell attached configuration.

^eRefers to slope of steady-state inactivation (h_∞) curve. Change in prepulse membrane potential (in mV) necessary to cause an e -fold reduction in the size of the response to a test pulse to 0 mV.

^fRefers to single-channel current amplitude in pA at 0 mV membrane potential. The respective chord conductances, assuming a reversal potential of -100 mV are 7.1 and 7.8 pS respectively.

^gRefers to time constant of recovery from inactivation at -40 mV membrane potential as measured in a two pulse experiment. Both test pulses were from a hold potential from -80 to $+20$ mV with a duration of 120 ms. To estimate the time constant the times between the pulses was varied.

Implications for K^+ channel structure

The sequences of voltage-gated K^+ channels which have been cloned and expressed so far indicate that these channels have a common architectural design (Stühmer *et al.*, 1989a; Butler *et al.*, 1989; Yokoyama *et al.*, 1989). Possibly, they possess six membrane-spanning helices which are oriented in a pseudosymmetric fashion across the membrane (see Figure 1). The N- and C-terminal ends would be located in this topology at the intracellular side. Two sequence motifs of five amino acids each are present in every K^+ channel sequence known so far. One sequence motif (EYFFD) is located 89 amino acids in front of segment S1; the other sequence motif (MTTVG) is located in the bend region

between proposed transmembrane segments S5 and S6 (Frech *et al.*, 1989; Yokoyama *et al.*, 1989). Given the topological model of K^+ channels (Figure 1), the EYFFD sequence motif is located intracellularly and the MTTVG sequence motif extracellularly. The ubiquitous occurrence of these two sequence motifs in K^+ channel sequences suggests that they fulfill an essential structural role in K^+ channel function. This proposition is supported by our finding that the *Sh^{KS133}* mutation has occurred in the MTTVG sequence. In the absence of structural information, we cannot exclude that the *Sh^{KS133}* mutation may result in an overall conformational change of the K^+ channel. However, *in vitro* mutagenesis studies on the charybdotoxin

Table II. Pharmacological properties of *ShA2* and *Sh⁵A2* K⁺ channels

	DTX (nM)	MCDP (nM)	TEA (mM)	4-AP (mM)	CTX (nM)
<i>ShA2</i>	>>200	>>1000	17.8	5.5	4.0
<i>Sh⁵A2</i>	>>200	>>1000	13.8	2.7	5.5

Doses of various K⁺ channel blockers and toxins giving a 50% reduction in outward K⁺ currents recorded after 50 ms of a depolarizing pulse of +20 mV. Currents were recorded using a standard two electrode voltage clamp from oocytes bare of their vitelline envelope. DTX and MCDP did not show an effect at the concentrations given. Values reported are from fits of various inhibition doses to a dose-response function. Before each measurement, 10 identical depolarizations to +20 mV, each one lasting 50 ms were applied to equilibrate for use dependence.

binding site of *Sh* K⁺ channels (MacKinnon and Miller, 1989) have indicated that a glutamate residue (E422 of *ShA2*) is some 10–20 Å distant from the K⁺ channel binding site for charybdotoxin. This toxin blocks K⁺ permeation through the pore of the channel (MacKinnon and Miller, 1989). 18 amino acids away from this glutamate residue occurs the MTTVG sequence motif. We propose that this highly conserved K⁺ channel sequence motif is near or in the externally facing mouth of the K⁺ conduction pathway. Accordingly, the aspartate residue in *Sh^{KS133}* K⁺ channels would obstruct K⁺ permeation through the pore.

The *Sh⁵* mutation replaces within the proposed transmembrane segment S5 the aromatic amino acid phenylalanine by the aliphatic amino acid isoleucine at a site which is highly conserved within the K⁺ channel superfamily (Yokoyama *et al.*, 1989). This inconspicuous structural alteration has profound effects on the electrophysiological properties of the *Sh* K⁺ channels. The voltage dependence of activation and inactivation, the rate of activation as well as the rate of recovery from inactivation is accelerated in *Sh⁵* channels. The changes of these seemingly different properties of the *Sh* K⁺ channel strongly suggest that the *Sh⁵* mutation induces a conformational change. It has been proposed that segment S5 is connected with segment S4, the probable voltage sensor of the channel (Stühmer *et al.*, 1989b), via a leucine zipper motif (MacCormack *et al.*, 1989). Transcription factors containing a leucine zipper motif possibly dimerize through leucine–leucine interaction (Landschütz *et al.*, 1988). This dimerization requires the parallel opposition of two linear arrays of leucine heptad repeats (Abel and Maniatis, 1989). Based on the proposed topology of *Sh* K⁺ channel subunits, the K⁺ channel leucine heptad repeat might form a leucine zipper with adjacent subunits via an intermolecular interaction. Such an interaction could be responsible for a link between the voltage sensing part (segment S4) of the K⁺ channel and the *Sh⁵* mutation in segment S5. Thereby, voltage dependence and gating behaviour of *Sh⁵* K⁺ channels might be altered in concert.

Sh^{E62} and the organization of 3' splice site sequences

The sequences required for splicing in higher eukaryotes include conserved elements at the 5' and 3' splice sites and a less conserved element, the branchpoint sequence, at the site of lariat formation (for review see Steitz *et al.*, 1988). Splicing usually takes place at the first AG downstream from the branch site (Reed and Maniatis, 1985). In most introns, a pyrimidine residue is located immediately upstream of the

AG, adenine residues occur less frequently, and guanine residues are rare (Mount, 1982). It is surprising, therefore, that *Sh^{E62}* RNA is not spliced between exons 19 and 20 although the acceptor site AG is shifted one nucleotide downstream because the sequence AGG (*Sh⁺*) has been mutated at AAG (*Sh^{E62}*). Similarly, mutation of CAG to AAG in rabbit globin intron 2 leads to a substantial reduction in the efficiency of lariat formation (Aebi *et al.*, 1986). Apparently, the sequence between branchpoint and 3' acceptor site plays an important role in the efficiency of the splicing reaction (Reed, 1990). In this context, it should be noted that the acceptor site sequence in front of exon 17 of *Sh⁺* RNAs is AGAG. In this case, the second, and not the first AG is used as 3' acceptor in the natural splicing reaction indicating that a simple scanning mechanism between branchpoint and 3' acceptor site does not apply.

Materials and methods

Sequencing of mutant DNA

Wild type DNA of the *Sh* locus has been isolated and sequenced as described (Pongs *et al.*, 1988). Genomic *Sh⁵* and *Sh^{KS133}* libraries were prepared with partial *Mbo*I or *Eco*RI digests of adult DNA inserted into cosPneo cosmid vector (Steller and Pirotta, 1985). Restriction fragments of recombinant cosmids containing exons 7–15 of the *Sh* transcription unit were subcloned into Bluescript (Stratagene) by standard cloning techniques. *Sh^{E62}* DNA was digested with *Bam*HI or with *Eco*RI/*Hind*III followed by gel electrophoresis of the resulting fragments on 0.8% agarose gels (Maniatis *et al.*, 1982). Restriction fragments of the expected size according to the restriction map of the *Sh* locus (map coordinates +18 to +34.5, +32.8 to +37.3) were isolated. Isolated fragments were ligated with corresponding arms of EMBL3 or NM1149 vector (Murray, 1983). Recombinant phages containing *Sh^{E62}* DNA encoding exons 16–18 and 19–21 of the *Sh* transcription unit (Pongs *et al.*, 1988) were isolated. DNA was subcloned into Bluescript (Stratagene). Sequencing of both strands was done according to Sanger *et al.* (1977) using T7 Sequencing™ kit (Pharmacia LKB Biotechnology AG) or Sequenase™ kit (USB Corporation).

In vitro mutagenesis

For cRNA synthesis *ShA2* was cloned in the expression vector pAS18 (Stocker *et al.*, 1990). The *Sh⁵* and *Sh^{KS133}* mutations were introduced into *ShA2* cDNA (Baumann *et al.*, 1989) with the oligonucleotide priming technique (Kramer *et al.*, 1984). Corresponding primers for the two mutations were: GGTTTACTTATAATTTCTTATTTATAGG (*Sh⁵*) and CCATGACCACCGATGGATATGGTG (*Sh^{KS133}*). The *in vitro* mutagenesis was carried out with the site directed mutagenesis kit (Boehringer Mannheim, FRG).

Sh⁵A2 and *Sh^{KS133}A2* were cloned into the *Sma*I restriction site of the expression vector pAS18. For cloning *ShA1* and *Sh^{E62}* we constructed a pAS18- α_E clone. This clone was obtained by ligating the *Xba*I–*Eco*RI fragment of cDNA α (nt 735–2316 in Pongs *et al.*, 1988) with *Xba*I/*Sma*I cut pAS18 after filling in the *Eco*RI site with DNA polymerase I (Klenow). The construction of pAS18- α_E allowed us to ligate with *Hind*III/*Xba*I cut pAS18- α_E the N-terminus of *ShA1* protein. For this purpose the *Hind*III site was filled in with DNA polymerase I (Klenow). pAS18-A1 was obtained by ligating the *Hind*III/*Xba*I cut pAS18- α_E DNA with the *Eco*RI–*Xba*I fragment of cDNA α (nt –406 to 735 in Pongs *et al.*, 1988) after filling in its *Eco*RI site. The *Sh^{E62}* mutation was introduced into pAS18-*ShA1* which was cut with *Asp*718 and *Sac*I. It was ligated with an *Asp*718–*Bgl*III *Sh^{E62}* DNA restriction fragment containing sequences from exon 19 to exon 20 (see Figures 3 and 4) in order to replace the 3'-terminus of *ShA1* with the corresponding *Sh^{E62}* 3'-terminus. Before ligation the *Sac*I site of cut pAS18-*ShA1* was filled in with T4 DNA polymerase as well as the *Bgl*III site of the *Sh^{E62}* DNA restriction fragment.

The mutations *Sh^{KS133}A2*, *Sh⁵A2*, *Sh^{E62}A1* were controlled by sequencing the entire coding regions.

Polymerase chain reactions

mRNA isolated from adult heads (*Sh^{E62}* or *Sh⁺*) was transcribed *in vitro* into cDNA using a cDNA synthesis kit (Boehringer Mannheim). Polymerase chain reactions with genomic DNA or cDNA (Saiki *et al.*, 1985) were performed with GeneAmp™ DNA Amplification Reagent Kit (Perkin

Elmer Cetus) in a Perkin Elmer DNA Thermal Cycler (1 min 57°C, 2 min 72°C, 1 min 92°C, 30 cycles). The reaction was primed with primers complementary to sequences in exon 19 (primer 1: CAACCACGT-TACAAGTTGTTTC) and exon 21 (primer 2: CAAGCTGCGTGAAGT-GCACTG).

cRNA synthesis and injection into oocytes

cRNA was prepared from cDNA as described in Stühmer *et al.* (1988). After storage at -20°C the cRNA (0.4 mg/ml) was injected into oocytes of *X. laevis* (stage Vb/VI) in portions of ~50 nl/oocyte. The expression of *ShA2*, *ShA1* and *Sh⁵A2* channels was detectable in nearly every oocyte on the second day after injection. Our nomenclature of *Sh K⁺* channel forming proteins has been described in Baumann *et al.* (1989). *ShA1* corresponds to *ShA* of Schwarz *et al.* (1988) and *ShA2* to *ShB* of Schwarz *et al.* (1988). *ShA1* and *ShA2* proteins possess the same N-terminal sequence ('A'), but differ in their C-termini as indicated by the number.

Current recording

Experiments were carried out in normal frog ringer containing (in mM) NaCl 115, KCl 2.5, CaCl₂, 1.8 HEPES 10 (pH 7.2). In some cases, sodium was partially replaced by the blocking substances 4-aminopyridine (4-AP) and tetraethylammonium chloride (TEA) (Sigma). Dendrotoxin (DTX), mast cell degranulating peptide (MCDP) (gifts from Drs F.Dreyer and E.Habermann, Universität Giessen, FRG) and charybdotoxin (CTX) (gift from Dr C.Miller, Brandeis University, USA) were added to the bathing solution.

Whole cell currents were recorded using a two microelectrode voltage clamp circuit. Both current and voltage pipettes were filled with 3 M KCl and had resistances of 0.5–1 MΩ. The recovery of inactivation was measured by this configuration. To estimate τ the function $I/I_{\max} = c_0 - c_1 \cdot \exp(t/\tau)$ was fitted to the peak maxima at various times. c_0 equals maximal recovery; c_1/I_{\max} at $t = 0$.

Pipettes for macro-patches were made from aluminium silicate glass and had a tip diameter of ~4.6 μm (Stühmer *et al.*, 1987). They were filled with the normal bathing solution for cell-attached recording giving a resistance of 0.5–1 MΩ. The intracellular potential was simultaneously measured by a microelectrode to determine the effective transmembrane potential across the patch. The K⁺ channel density was not homogeneous and therefore the oocyte had to be patched on several different places before finding an area of high current density. Stimulation and sampling were done as described (Stühmer *et al.*, 1985). To determine the steady-state activation parameters, the function $G = G_{\max}/[1 + \exp\{(V_{1/2} - V)/a\}]$ was fitted to the conductance values at each potential. These conductances were obtained by dividing the peak current by the driving force, assuming a reversal potential of -100 mV in the cell-attached configuration and a calculated reversal of -98 mV in the inside-out configuration. Steady-state inactivation parameters were measured only for the channel inactivating in the ms time scale, *ShA2*, using prepulses lasting 1 s. The data was analysed by fitting the function $I/I_{\max} = 1/[1 + \exp\{(V - V_{1/2})/a\}]$ to the data points. Pipettes for single-channel recordings were made from borosilicate glass and had resistances of 3–5 MΩ when filled with bathing solution. The single-channel current records were stored on video tape and analysed by an interactive semi-automatic procedure. Distributions of single-channel current amplitudes were fitted assuming Gaussian distribution.

Acknowledgements

We thank Drs F.Dreyer and E.Habermann for the generous gift of DTX and MCDP and Dr C.Miller for the generous gift of CTX. This work was supported by the Leibniz-Förderprogramm (to Dr E.Neher) and grants from the Deutsche Forschungsgemeinschaft (G.Boheim and O.Pongs), the Volkswagen Stiftung (A.Ferrus and O.Pongs), CAYCIT (A.Ferrus).

References

- Abel, T. and Maniatis, T. (1989) *Nature*, **341**, 24–25.
 Abrams, T.W. and Kandel, E.R. (1988) *Trends Neurosci.*, **11**, 128–135.
 Aebi, M., Hornig, H., Padgett, R.A., Reiser, J. and Weissmann, C. (1986) *Cell*, **47**, 555–556.
 Barbas, J.A., Rubio, N., Pedrosa, E., Pongs, O. and Ferrus, A. (1989) *Mol. Brain Res.*, **5**, 171–176.
 Baumann, A., Krah-Jentgens, I., Müller, R., Müller-Holtkamp, F., Canal, I., Galceran, J., Ferrus, A. and Pongs, O. (1989) In Maelicke, A. (ed.), *Molecular Biology of Neuroreceptors and Ion Channels*. Springer-Verlag, Heidelberg, pp. 231–243.
 Butler, A., Wei, A., Baker, K. and Salkoff, L. (1989) *Science*, **243**, 943–947.

- Crow, T. (1988) *Trends Neurosci.*, **11**, 136–142.
 Ferrus, A., Barbas, J.A., Galceran, J., Krah-Jentgens, I., de la Pompa, J.L., Canal, I. and Pongs, O. (1990) *Genetics*, **125**, 383–398.
 Frech, G.C., Van Dongen, A.M.J., Schuster, G., Brown, A.M. and Joho, R.M. (1989) *Nature*, **340**, 642–645.
 Gisselmann, G., Sewing, S., Madsen, B.W., Mallart, A., Angaut-Petit, D., Müller-Holtkamp, F., Ferrus, A. and Pongs, O. (1989) *EMBO J.*, **8**, 2359–2364.
 Haugland, F.N. and Wu, C.F. (1990) *J. Neurosci.*, **10**, 1357–1371.
 Hille, B. (1984) *Ionic Channels of Excitable Membranes*. Sinauer Sunderland, Massachusetts.
 Iverson, L.E., Tanouye, M.A., Lester, H.A., Davidson, N. and Ruby, B. (1988) *Proc. Natl. Acad. Sci. USA*, **85**, 5723–5727.
 Kamb, A., Iverson, L.E. and Tanouye, M.A. (1987) *Cell*, **50**, 405–413.
 Kamb, A., Tseng-Crank, J. and Tanouye, M.A. (1988) *Neuron*, **1**, 421–430.
 Kramer, W., Drutsa, V., Jansen, H.W., Kramer, B., Pflugfelder, M., and Fritz, H.J. (1984) *Nucleic Acids Res.*, **12**, 9441–9456.
 Lanschütz, W.H., Johnson, P.F. and McKnight, S.L. (1988) *Science*, **240**, 1759–1764.
 MacKinnon, R. and Miller, C. (1989) *Science*, **245**, 1382–1385.
 Maniatis, T., Fritsch, E.F. and Sambrook, J. (1982) *Molecular Cloning. A Laboratory Manual*. Cold Spring Harbor Laboratory Press, Cold Spring Harbor, NY.
 McCormack, K., Campanelli, J.T., Ramaswami, M., Mathew, M.K. and Tanouye, M. (1989) *Nature*, **340**, 103.
 Mount, S.M. (1982) *Nucleic Acids Res.*, **10**, 459–472.
 Murray, N. (1983) In Hendrix, R.W., Roberts, J.W., Stahl, F. and Weisberg, R.A. (eds) *Lambda II*. Cold Spring Harbor Laboratory Press, Cold Spring Harbor, NY, pp. 395–432.
 Pongs, O., Kecskemethy, N., Müller, R., Krah-Jentgens, I., Baumann, A., Kiltz, H.H., Canal, I., Llamazares, S. and Ferrus, A. (1988) *EMBO J.*, **7**, 1087–1097.
 Reed, R. (1990) *Genes Dev.*, **3**, 2113–2123.
 Reed, R. and Maniatis, T. (1985) *Cell*, **41**, 95–105.
 Saiki, R.K., Schorf, S., Faloona, F., Mullis, K.B., Horn, G.T., Ehrlich, H.A. and Arnheim, N. (1988) *Science*, **230**, 1350–1354.
 Sanger, F., Nicklen, S. and Coulson, A.R. (1977) *Proc. Natl. Acad. Sci. USA*, **74**, 5463–5467.
 Salkoff, L. (1983) *Cold Spring Harbor Symp. Quant. Biol.*, **48**, 221–231.
 Schwarz, T., Tempel, B.L., Papazian, D.M., Jan, N.J. and Jan, L.Y. (1988) *Nature*, **331**, 137–142.
 Solc, C.K., Zagotta, W.N. and Aldrich, R.W. (1987) *Science*, **236**, 1094–1098.
 Steitz, J.A., Black, D.L., Gerke, V., Parker, K.A., Kramer, A., Frensdewey, D. and Keller, W. (1988) In Birnstiel, M.L. (ed.) *Structure and Function of Major and Minor SNURPS*. Springer Verlag, Heidelberg, pp. 115–154.
 Steller, H. and Pirotta, V. (1985) *EMBO J.*, **4**, 167–171.
 Stocker, M., Stühmer, W., Wittka, R., Wang, X., Müller, R., Ferrus, A. and Pongs, O. (1990) *Proc. Natl. Acad. Sci. USA*, in the press.
 Stühmer, W., Methfessel, C., Sakmann, B., Noda, M. and Numa, S. (1985) *Eur. Biophys. J.*, **14**, 131–138.
 Stühmer, W., Stocker, M., Sakmann, B., Seeburg, P., Baumann, A., Grupe, A. and Pongs, O. (1988) *FEBS Lett.*, **242**, 199–206.
 Stühmer, W., Ruppersberg, J.P., Schröter, K.H., Sakmann, B., Stocker, M., Giese, K.P., Perschke, A., Baumann, A. and Pongs, O. (1989a) *EMBO J.*, **8**, 3235–3244.
 Stühmer, W., Conti, F., Suzuki, H., Wang, X., Noda, M., Yahagi, M., Kubo, H. and Numa, S. (1989b) *Nature*, **339**, 597–609.
 Tanouye, M.A. and Ferrus, A. (1985) *J. Neurogenet.*, **2**, 253–271.
 Tanouye, M.A., Ferrus, A. and Fujita, S.C. (1981) *Proc. Natl. Acad. Sci. USA*, **78**, 6548–6552.
 Timpe, L.C. and Jan, L.Y. (1987) *J. Neurosci.*, **7**, 1307–1317.
 Timpe, L.C., Schwarz, T.L., Tempel, B.L., Papazian, D.M., Jan, Y.N. and Jan, L.Y. (1988a) *Nature*, **331**, 143–145.
 Timpe, L.C., Jan, Y.N. and Jan, L.Y. (1988b) *Neuron*, **1**, 659–667.
 Wu, C.F. and Haugland, F.N. (1985) *J. Neurosci.*, **5**, 2626–2640.
 Yokoyama, S., Imoto, K., Kawamura, T., Higashida, A., Iwabe, N., Miyata, T. and Numa, S. (1989) *FEBS Lett.*, **259**, 37–42.
 Zagotta, W. and Aldrich, R. (1990) *J. Neurosci.*, **10**, 1799–1810.

Received on July 10, 1990; revised on September 10, 1990

Note added in proof

Our observations and conclusions and the *Sh⁵* mutation are in accord with those reported by M.Gautam and M.A.Tanouye which appeared in *Neuron* **5** (1990), 76–73 after submission of this paper.